

DETECTION OF COSMIC SHEAR WITH THE *HST* SURVEY STRIP

JASON RHODES^{1,2}, ALEXANDRE REFREGIER³ & EDWARD J. GROTH²

1 Code 681, Goddard Space Flight Center, Greenbelt, MD 20771; jrhodes@band1.gsfc.nasa.gov

2 Physics Department, Princeton University, Jadwin Hall, P.O. Box 708, Princeton, NJ 08544; groth@pupgg.princeton.edu

3 Institute of Astronomy, Madingley Road, Cambridge, CB3 OHA, U.K.; ar@ast.cam.ac.uk

Submitted to *ApJ* January 12, 2001

ABSTRACT

Weak lensing by large-scale structure provides a unique method to directly measure matter fluctuations in the universe, and has recently been detected from the ground. Here, we report the first detection of this ‘cosmic shear’ based on space-based images. The detection was derived from the Hubble Space Telescope (HST) Survey Strip (or “Groth Strip”), a $4' \times 42'$ set of 28 contiguous WFPC2 pointings with $I < 27$. The small size of the HST Point-Spread Function (PSF) affords both a lower statistical noise, and a much weaker sensitivity to systematic effects, a crucial limiting factor of cosmic shear measurements. Our method and treatment of systematic effects were discussed in an earlier paper (Rhodes, Refregier & Groth 2000). We measure an rms shear of 1.8% on the WFPC2 chip scale ($1.27'$), in agreement with the predictions of cluster-normalized CDM models. Using a Maximum Likelihood (ML) analysis, we show that our detection is significant at the 99.5% confidence level (CL), and measure the normalization of the matter power spectrum to be $\sigma_8 \Omega_m^{0.48} = 0.51_{-0.17}^{+0.14}$, in a Λ CDM universe. These 68% CL errors include (Gaussian) cosmic variance, systematic effects and the uncertainty in the redshift distribution of the background galaxies. Our result is consistent with earlier lensing measurements from the ground, and with the normalization derived from cluster abundance. We discuss how our measurement can be improved with the analysis of a large number of independent WFPC2 fields.

Subject headings: cosmology: observations - gravitational lensing - cosmology: large-scale structure of universe - cosmology: dark matter

1. INTRODUCTION

Weak gravitational lensing has now been established as a unique technique to measure the mass distribution in the universe (see Mellier 1999; Bartelmann & Schneider 2000 for reviews). Recently, several groups detected this effect in the field by measuring the coherent distortions it induces in the shape of background galaxies (Wittman et al. 2000; van Waerbeke et al. 2000; Bacon, Refregier & Ellis 2000a (BRE); Kaiser, Wilson & Luppino 2000; Maoli et al. 2000). This opens wide prospects for the measurement of the distribution of dark matter on cosmological scales and of cosmological parameters.

In this paper, we present the first detection of this ‘cosmic shear’ based on space-based images. For this purpose, we use the HST Survey Strip (or “Groth Strip”), a $4' \times 42'$ survey consisting of 28 contiguous WFPC2 fields with a limiting magnitude of $I \approx 27$ (Groth et al. 1994). A shear measurement method adapted to HST images and a detailed study of systematic effects for the Strip was presented in an earlier paper Rhodes, Refregier & Groth (2000, RRG; see also Rhodes 1999). The main advantage of HST images for weak lensing is the small PSF ($0.1''$ compared to $\sim 1''$ from the ground), which allows a larger surface density of resolved galaxies and makes the shear measurement much less sensitive to the PSF smearing. We apply the results to the Strip and search for a lensing signal using a Maximum Likelihood (ML) approach. We then derive constraints on the amplitude of the mass power spectrum and compare it to other measurements.

The paper is organized as follows. In §2 we summarize the main theoretical results which serve as a reference for

our measurement. In §3 we describe the relevant properties of our data set. Our method for measuring the shear and our treatment of systematic effects are described in §4. Our results are presented in §5 and discussed and summarized in §6.

2. THEORY

We measure the average shear $\bar{\gamma}_i$ within each WFPC2 chip, which are square cells of side $\alpha = 1.27'$. The angular fluctuations of the resulting smoothed shear field are characterized by the shear correlation functions $C_i(\theta) \equiv \langle \bar{\gamma}_i^r(0) \bar{\gamma}_i^r(\theta) \rangle$, where $i = 1, 2$ and the brackets refer to an average over pair of cells separated by an angle $\theta = |\theta|$. The shear components $\bar{\gamma}_i^r$ are measured in a rotated coordinate system whose x -axis is aligned with the separation vector θ between the two points (see e.g. Heavens, Refregier & Heymans 2000). These correlation functions can be computed for any cosmological model using (see eg. BRE)

$$C_i(\theta) = \frac{1}{4\pi} \int_0^\infty l C_l \left| \widetilde{W}_l \right|^2 [J_0(l\theta) \pm J_4(l\theta)], \quad i = 1, 2, \quad (1)$$

where \widetilde{W}_l is the window function of a square cell. The shear power spectrum C_l is defined as in BRE and can be evaluated from the evolution of the non-linear matter power spectrum using the fitting formula from Peacock & Dodds (1997). In this paper, we will consider a Λ CDM model with $\Omega_m = 0.3$, $\Omega_\Lambda = 0.7$, $\Gamma = 0.25$, and consider several values of σ_8 , the normalization of the mass fluctuations on $8 h^{-1}$ Mpc scales.

The variance of the cell-averaged shear is $\sigma_{\text{lens}}^2 \equiv \langle |\bar{\gamma}|^2 \rangle = C_1(0) + C_2(0)$. For the Λ CDM model, the rms shear in a cell is

$$\sigma_{\text{lens}} \simeq 0.0197 \left(\frac{\sigma_8}{1} \right)^{1.24} \left(\frac{\Omega_m}{0.3} \right)^{0.60} \left(\frac{z_m}{0.9} \right)^{0.85}, \quad (2)$$

where z_m is the median redshift of the background galaxies, whose redshift distribution was taken to be of the form of Equation (3) below. The scaling relations in Equation (2) provide an excellent approximation in our range of interest, namely, $0.6 \lesssim \sigma_8 \lesssim 1.4$ and $0.7 \lesssim z_m \lesssim 1.2$.

3. DATA

The Hubble Space Telescope Survey Strip (sometimes referred to as the ‘Groth Strip’, or the ‘Groth-Westphal Strip’) was taken during March and April 1994 using the Guaranteed Time Observations of one of us (EJG) and the WFPC-1 Instrumentation Definition Team (Groth et al. 1994). The Strip was observed in two passbands, V (F606W) and I (F814W). For 27 of the pointings in the Strip, total exposure times were 2800 and 4400 seconds in the V and I bands, respectively. One of the Strip pointings (the Strip Deep Field) had exposure times of 24,400 and 25,200 seconds, arranged in 4 dithers. We used only the I-band images to study weak lensing. The Strip images consist of 4 individual exposures with equal exposure times. Here, we chose to use only one of the four dithers for the Deep Field, thus avoiding the complications in the PSF correction that dithering would introduce (see RRG).

We used the Faint Object Classification and Analysis System (FOCAS; Jarvis and Tyson, 1981) within IRAF to create a catalog of objects in the Strip. We determine the sky background and its standard deviation using the IRAF task `Imarith`. This was found to be more reliable than the corresponding algorithm within FOCAS. Magnitude zero points are those defined by Holtzman et al. (1995). A FOCAS catalog was created for each filter, and a matched catalog was created for objects that had I and V positions that coincided within a radius of about 5 pixels. There were approximately 10,000 matched objects with $I < 26$. Of these objects, approximately 4000 were classified as galaxies, had well defined moments and were sufficiently large to be used in our weak lensing study. We were careful not to double count galaxies that fall in the small overlap region between consecutive fields in the Strip.

Koo et al. (1996) have shown that a small subsample (24 galaxies) of Strip objects matches an extrapolation of the CFRS sample redshift distribution. More recent redshift measurements of galaxies in the Strip by the DEEP collaboration (DEEP Collaboration, 1999) agree with the preliminary findings in Koo et al. (1996). Assuming the functional form of the redshift distribution found in the CFRS,

$$\frac{dN}{dz} \propto z^2 e^{-(z/z_o)^2} \quad (3)$$

and using the median redshift of $z_m \simeq z_o = 0.5$ for objects in the range $17 < I < 22$ found in that survey (Lilly et al. 1995), we calculate a median redshift for objects in the Strip. The galaxy sample we use to study weak

lensing ($I < 26$ and size $d > 1.5$ pixels) has a median magnitude of $I = 23.6$. Extrapolating from the CFRS sample using the Strip number counts, this corresponds to a median redshift of $z_m = 0.9$ (Rhodes 1999, Groth and Rhodes, 2001). Photometric redshifts for galaxies in the Hubble Deep Fields (HDF-North and HDF-South) have been measured by Lanzetta et al. (1996). A linear fit to the median redshift versus median magnitude plot yields $z_m = 0.87$ for the HDF-South and $z_m = 1.00$ for the HDF-North for a median magnitude of $I = 23.6$, where we have used the magnitude conversion $I = -0.49 + I_{AB}$. This is consistent with what we found above using an extrapolation of the CFRS sample. Therefore, we adopt a median redshift of $z_m = 0.9 \pm 0.1$ for the lensing analysis in this paper.

4. PROCEDURE AND SYSTEMATIC EFFECTS

The procedure we use for extracting galaxy ellipticities and shear from the source images is described in detail in RRG (see also Rhodes 1999). This method is based on one introduced by Kaiser, Squires, and Broadhurst (KSB, 1995), but modified and tested for application to HST images. The KSB method was shown to be adequate for current ground based surveys (Bacon, et al. 2000b; Erben et al. 2000). In RRG, we used numerical simulations and an array of tests to show that our method was sufficiently accurate for WFPC2 images.

We use our method to correct for two effects: camera distortion and convolution with the anisotropic PSF. Corrections are done using moments measured with a Gaussian weight function whose size in pixels, ω , depends on the size of the object as $\omega = \max(2, \sqrt{A/\pi})$, where A is the area of the object in pixels. The minimum size of two pixels was found to be the optimal weight function size for stellar objects using both actual WFPC2 data and simulations using artificial stellar images created using the program Tiny Tim (Krist and Hook 1997).

Camera distortions are corrected using a map derived from stellar astrometric shifts (Holtzman, et al., 1995). PSF corrections are determined from HST observations of two globular clusters (M4 and NGC6572). Finally, we measure the ellipticities (ϵ_i) of the galaxies in the Strip and convert them into shear estimates using $\gamma_i = G^{-1}\epsilon_i$, where G is the shear susceptibility factor given by Eq. (30) in RRG.

RRG have shown that the residual systematic effects can be greatly minimized if (1) the shear is averaged over entire chips, and (2) only “large” galaxies with a (convolved) rms radius greater than 1.5 pixels (or about 0.15”) are selected. Since the PSF anisotropy is mainly tangential about the chip centers, condition (1) ensures that the mean PSF ellipticity is small ($\epsilon^* \sim 0.02$). Since the shapes of larger galaxies are less affected by the PSF, condition (2) ensures that the impact of the PSF anisotropy on galaxy ellipticities ϵ^g is small. Specifically, RRG show that the ellipticity of the selected galaxies ϵ_g induced by the PSF ellipticity is reduced by a factor $f_{\text{red}} \equiv \epsilon^g/\epsilon^* \simeq 0.13$.

As shown in RRG, the residual systematics for this galaxy subsample are dominated by two effects. The first arises from the imperfect accuracy of the ellipticity corrections and shear measurement method. This effect results in an uncertainty in the normalization of the shear

of about 4% and is easily incorporated at the end of our analysis. The second results from the time variability of the PSF. To quantify this effect, we measure the mean ellipticity of the PSF in each chip for 4 stellar fields (M4 observed at 2 different epochs, NGC6572, and a stellar field from the WFPCC2 parallel archive). We find that the chip-averaged PSF ellipticity $\bar{\epsilon}_{ic}^*$ varies by about 0.01 (rms) in chips $c = 2$ and 3 and 0.02 in $c = 4$. The variations appear to be stochastic and to be unrelated to the focus position of the telescope. These time variations must be corrected statistically since the small number of stars in the Strip precludes measuring the PSF in each field individually. For this purpose, we measure the covariance $C_{ic, jc'}^* \equiv \text{cov}[\bar{\epsilon}_{ic}^*, \bar{\epsilon}_{jc'}^*]$ of the stellar ellipticities by averaging over all stellar fields, and convert this into the systematics shear correlation matrix $C_{ic, jc'}^{\text{sys}} \simeq f_{\text{red}}^{-2} G^{-2} C_{ic, jc'}^*$ which is subtracted from the galaxy shear correlation functions. The diagonal elements are the shear variance produced by the time variability of the PSF $\sigma_{\text{sys}}^2 = \langle C_{1c, 1c}^{\text{sys}} + C_{2c, 2c}^{\text{sys}} \rangle_c \simeq 0.0011^2$, where the average is over all chips.

5. RESULTS

To study the lensing statistics in the Strip, we first compute the mean shear $\bar{\gamma}_{ic}$ in each chip c , by averaging over all selected galaxies in the chip. This mean shear is the sum of contributions from lensing, noise and systematic effects, i.e. $\bar{\gamma}_{ic} = \bar{\gamma}_{ic}^{\text{lens}} + \bar{\gamma}_{ic}^{\text{noise}} + \bar{\gamma}_{ic}^{\text{sys}}$. From the distributions of the galaxy shears within each chip, we can measure the covariance matrix $C_{ic, jc'}^{\text{noise}} \equiv \text{cov}[\bar{\gamma}_{ic}^{\text{noise}}, \bar{\gamma}_{jc'}^{\text{noise}}]$ of the mean shear components. Since the chips do not overlap, $C_{ic, jc'}^{\text{noise}}$ vanishes for $c \neq c'$. The diagonal elements $C_{ic, ic}^{\text{noise}} \equiv \sigma_{\text{noise}, ic}^2$ are the errors in the mean for the mean shear components $\bar{\gamma}_{ic}$. The average noise variance is $\sigma_{\text{noise}}^2 \equiv \langle \sigma_{\text{noise}, 1c}^2 + \sigma_{\text{noise}, 2c}^2 \rangle_c \simeq 0.047^2$, where the average is over all chips. The off-diagonal entries in the noise matrix are an order of magnitude below the diagonal ones and thus do not have much impact on the analysis. We nevertheless keep them for completeness.

The shear pattern for the Strip is shown in Figure 1. Since the expected signal on the chip scale is about $\sigma_{\text{lens}} \simeq 0.02$ (see Eq.[2]), the signal-to-noise ratio $\sigma_{\text{lens}}/\sigma_{\text{noise}}$ for each chip is about 0.4. The lensing signal must therefore be searched for statistically. For this purpose, we first consider the mean shear $\langle \bar{\gamma}_{ic} \rangle_c$ averaged over all chips in the Strip. We find $\langle \bar{\gamma}_1 \rangle = 0.005 \pm 0.004$ and $\langle \bar{\gamma}_2 \rangle = 0.005 \pm 0.004$, where the errors are 1σ errors in the mean. This is consistent with zero, as expected given the length of the Strip. This nonetheless confirms that we are not subject to systematic effects on large scales.



Fig. 1.— The ellipticity of each field and chip in the Survey Strip. The Strip measures about 4 by 42 arcminutes.

We next consider the variance of the shear on the chip scale. In general, the total observed shear variance $\sigma_{\text{tot}}^2 \equiv \langle |\bar{\gamma}_{ic}|^2 \rangle$ is the sum of the contribution from lensing, from noise, and from systematic effects, i.e. $\sigma_{\text{tot}}^2 =$

$\sigma_{\text{lens}}^2 + \sigma_{\text{noise}}^2 + \sigma_{\text{sys}}^2$. An estimator for the lensing variance is thus $\sigma_{\text{lens}}^2 \simeq \sigma_{\text{tot}}^2 - \sigma_{\text{noise}}^2 - \sigma_{\text{sys}}^2$ (for more details, see BRE). Using our estimate of σ_{sys} (see §4), we find $\sigma_{\text{lens}} \simeq 0.018$, which is close to the expected value of 0.0197 in the Λ CDM model (see Eq. [2]). Estimating errors on the shear variance is complicated since the chips are contiguous and thus not independent. Instead of attempting to do this, we use a maximum likelihood approach to extract the lensing signal on all scales simultaneously.

To do so, we assume that the shear field obeys Gaussian statistics. Since we are averaging over a large number of galaxies (about 50) in each field, the central value theorem ensures that this assumption is valid for the noise contribution. It is difficult to establish whether the systematics are Gaussian; however, since they have a much smaller amplitude than the noise, it is sufficient to assume that they are so. The lensing shear field is known not to be Gaussian, especially on scales smaller than $10'$ which are dominated by the non-linear evolution of structures (Jain & Seljak 1997). However, as we have shown above, the noise dominates over the lensing signal in each individual chip. Therefore our Gaussian approximation should not underestimate our error bars by a large amount.

With this approximation, the probability of measuring the mean shears $\bar{\gamma}_{ic}$ given a cosmological model M is

$$P(\bar{\gamma}_{ic}|M) \simeq \frac{e^{-\frac{1}{2}g^T C^{-1} g}}{(2\pi)^N |C|^{\frac{1}{2}}} \quad (4)$$

where $N = 84$ is the number of chips, and $g = (\bar{\gamma}_{11}, \bar{\gamma}_{21}, \dots, \bar{\gamma}_{1N}, \bar{\gamma}_{2N})$ is the data vector composed of the $2N$ measured shears. The total correlation matrix C is given by $C = C^{\text{lens}} + C^{\text{noise}} + C^{\text{sys}}$. The systematics correlation matrix C^{sys} is computed as explained in §4, assuming that each field is independent as indicated by the stochastic nature of the PSF variations. The lensing correlation matrix C^{lens} depends on the cosmological model and can be computed by unrotating the rotated correlation functions $C_1(\theta)$ and $C_2(\theta)$ (Eq. 1). Following Bayes' postulate, the likelihood L of the model M given the data is then $L \propto P(\bar{\gamma}_{ic}|M)$, so that its logarithm is given by

$$-2 \ln L \simeq g^T C^{-1} g + \ln |C| + \text{constant.} \quad (5)$$

First, we test the null hypothesis, namely the absence of lensing corresponding to $C^{\text{lens}} = 0$. In this case, $C = C^{\text{noise}} + C^{\text{sys}}$ is a constant, and the log likelihood reduces to $-2 \ln L = \chi^2 + \text{constant}$, where $\chi^2 \equiv g^T C^{-1} g$. For the Strip, we find a reduced χ^2 of 1.31 with 2×84 degrees of freedom. The null hypothesis is thus ruled out at the 99.5% confidence level, thus establishing our detection of the lensing signal. Note that this null test does not rely on the assumption that the lensing shear field is Gaussian, because we have set it to zero in this case.

Now that we have established the presence of a lensing signal, we can compute the constraints our data impose on cosmological parameters. To do so, we compute the Maximum Likelihood (ML) estimator for $\sigma_8(\Omega_m/0.3)^{0.48}$. This was done by maximizing $\ln L$ (Eq. [5]), which was computed with C_{lens} matrices corresponding to different values of this parameter. To compute the error in σ_8 we performed 1000 random realizations of the Strip with shears

drawn from a multivariate Gaussian distribution with a covariance matrix given by $C = C^{\text{lens}} + C^{\text{noise}} + C^{\text{sys}}$ (with C^{lens} at the MLE value of $\sigma_8(\Omega_m/0.3)^{0.48}$ of the Strip).

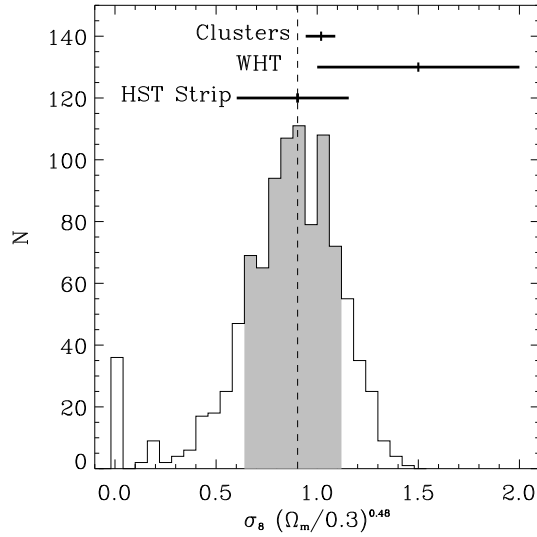


Fig. 2.— Distribution of the ML normalization of the power spectrum $\sigma_8\Omega_m^{0.48}$ derived from 1000 random realizations of the Strip. The normalization corresponding to the real Strip is shown as the vertical dashed line. The 68% confidence level is shown as the shaded region. The full 68% confidence interval which includes (Gaussian) cosmic variance, the uncertainty in the median redshifts of the background galaxies and that arising from systematic effects is shown as a horizontal bar. It can be compared to the corresponding limits derived from the William Herschel Telescope (WHT) cosmic shear survey of BRE, and to that from cluster abundance (Pierpaoli et al. 2000), shown as marked horizontal bars.

The resulting distribution of the ML values is shown in Figure 2. We thus obtain $\sigma_8(\Omega_m/0.3)^{0.48} = 0.90^{+0.22}_{-0.24}$ where the error bars correspond to the 68% confidence interval. After propagating errors induced by the uncertain median redshift z_m (see §3) of the galaxies and by the shear measurement method, our final 68% confidence range becomes $\sigma_8(\Omega_m/0.3)^{0.48} = 0.90^{+0.25}_{-0.30}$ and is shown as a horizontal bar in Figure 2. This value is consistent with the William Herschel Telescope (WHT) cosmic shear survey of BRE, who found $\sigma_8(\Omega_m/0.3)^{0.48} = 1.5 \pm 0.5$, as shown by the associated horizontal bar on the Figure. Our results are also consistent with the amplitude of the

cosmic shear signals found by other groups (Wittman et al. 2000; van Waerbeke et al. 2000; Kaiser et al. 2000; Maoli et al. 2000). However, since these groups do not include cosmic variance and redshift uncertainty in their error bar estimates, their results can not be directly compared with ours. The normalization from cluster abundance $\sigma_8(\Omega_m/0.3)^{0.60} = 1.019^{+0.070}_{-0.076}$ (Pierpaoli et al. 2000) is consistent with ours and is also shown on the figure (after ignoring the small difference in the exponents for Ω_m).

6. CONCLUSIONS

We have detected, for the first time, cosmic shear using space-based images. Our detection in the HST Survey Strip is significant at the 99.5% confidence level. Using a ML method to search for a lensing signal on all scales simultaneously, we derived a normalization of the matter power spectrum of $\sigma_8\Omega_m^{0.48} = 0.51^{+0.14}_{-0.17}$. This 68% confidence interval includes statistical noise, (Gaussian) cosmic variance, uncertainty in the redshift distribution of the galaxies and in our shear measurement method. This is consistent with ground-based cosmic shear surveys and with the normalization derived from cluster abundance.

Our result demonstrates the power of space-based images to measure cosmic shear. The small PSF in HST images affords both a larger surface density of background galaxies and a much reduced impact of the systematics induced by the PSF anisotropy. The latter advantage will be even more important for future, wider surveys whose sensitivity will be comparable to the amplitude of the systematics.

Our current results are chiefly limited by the relatively small area of the Strip. The signal-to-noise ratio for the detection of cosmic shear in N_f independent WFPC2 fields, in which we cannot search for lensing on all scales simultaneously as we have done here, is approximately $\text{S/N} \simeq (\sigma_{\text{lens}}/\sigma_{\text{noise}})^2 (3N_f)^{\frac{1}{2}} \simeq 6.8(N_f/500)^{\frac{1}{2}}$ (see BRE). Our detection can thus be significantly improved in the future by an analysis of existing disjoint WFPC2 fields.

We thank David Bacon for useful discussions. JR was supported by NASA Grant NAG5-6279 and a National Research Council-GSFC Research Associateship. AR was supported by a EEC fellowship from the TMR Gravitational Lensing Network and by a Wolfson College Research Fellowship. EJG was supported by NASA Grant NAG5-6279. We thank the WFPC1 IDT for their cooperation.

REFERENCES

Bacon, D.J., Refregier, A., & Ellis, R.S., 2000a (BRE), MNRAS, 318, 625
 Bacon, D.J., Refregier, A., Clowe, D., & Ellis, R.S., 2000b, submitted to MNRAS, preprint astro-ph/0007023
 Bartelmann, M., & Schneider, P., 2000, preprint astro-ph/9912508
 DEEP Collaboration, 1999, Private Communication
 Erben, T., van Waerbeke, L., Bertin, E., Mellier, Y., & Schneider, P., submitted to A&A, preprint astro-ph/0007021
 Groth, E. J., et al., 1994, BAAS, 26, 1403
 Groth, E. J., and Rhodes, J. 2001, In Preparation
 Heavens, A., Refregier, A., & Heymans, C., 2000, MNRAS, 319, 649
 Holtzman, J.A., et al. 1995, PASP, 107, 156
 Jain, B. & Seljak, U. 1997 ApJ, 484, 560
 Jarvis, J.F., & Tyson, J.A., 1981, AJ, 86, 476
 Kaiser, N., & Squires, G., & Broadhurst, T. 1995, ApJ, 449, 460
 Kaiser, N., Wilson, G., & Luppino, G.A., 2000, submitted to ApJLetters, preprint astro-ph/0003338
 Koo, D., et al. 1996, ApJ, 469, 535
 Krist, J., & Hook, R., 1997, The Tiny Tim User's Guide (Baltimore: STScI)
 Lanzetta, K., Yahil, A., & Fernandez-Soto, A., 1996, Nature, 381, 759 and data at <http://www.ess.sunysb.edu/astro/>
 Lilly, S., et al. 1995, ApJ455, 108
 Maoli, R., van Waerbeke, L., Mellier, Y., Schneider, P., Jain, B., Bernardeau, F., Erben, T., & Fort, B., 2000, submitted to A&A, preprint astro-ph/0011251
 Mellier, Y., 1999, ARA&A, 37, 127
 Peacock, J., & Dodds, S.J., 1997, MNRAS, 280, L19
 Pierpaoli, E., Scott, D., & White, M., 2000, submitted to MNRAS, preprint astro-ph/0010039
 Rhodes, J., 1999, PhD Thesis, Department of Physics, Princeton University

Rhodes, J., Refregier, A., & Groth, E.J., 2000, (RRG), ApJ, 536,
79
van Waerbeke, L., et al. 2000, A&A, 358, 30

Wittman, D.M., Tyson, J.A., Kirkman, D., Dell'Antonio, Ian, &
Bernstein, G., 2000, Nature, 405, 143